KI and TEDA influences towards the retention of radiotoxic CH3I by activated carbons

H. Lin, M. Chebbi, C. Monsanglant-Louvet, B. Marcillaud, A. Roynette, D. Doizi, P. Parent, C. Laffon, O. Grauby, Daniel Ferry

KI and TEDA influences towards the retention of radiotoxic CH_3I by activated carbons

H. Lin[1], M. Chebbi[1], C. Monsanglant-Louvet[1], B. Marcillaud[1], A. Roynette[1], D. Doizi[2], P. Parent[3], C. Laffon[3], O. Grauby[3], D. Ferry[3]*

[1] *Institut de Radioprotection et de Sûreté Nucléaire (IRSN), PSN-RES, Saclay, 91192 Gif-sur-Yvette, France*

[2] *Commissariat à l'Énergie Atomique (CEA), DEN/DES/ISAS/DPC/SECR/LRMO, Gif-sur-Yvette, 91191, France*

[3] *Aix Marseille University, CNRS, CINaM, Marseille, France*

* Corresponding author:

mouheb.chebbi@irsn.fr

GRAPHICAL ABSTRACT:

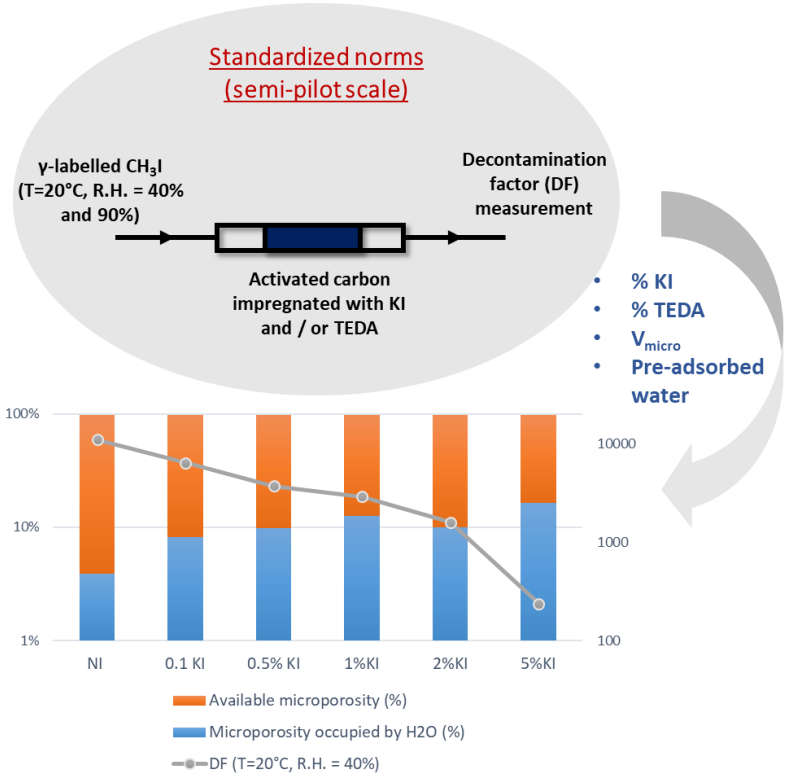

HIGHLIGHTS:

- Up to 21 AC are investigated for the capture of γ-CH_3I using standardized tests.
- Micropore blocking phenomena are only observed for high molar impregnation ratio.
- TEDA/AC display the best retention performances whatever the studied condition.
- The pre-adsorbed water governs the γ-CH_3I trapping for KI/AC at R.H. = 40%.

- A slight increase of DF is obtained as a function of KI content at R.H. = 90%.

KEYWORDS:

activated carbon, methyl iodide adsorption, decontamination factor, TEDA, KI

ABSTRACT

Activated carbons (AC) are widely used within the ventilation networks of nuclear facilities to trap volatile iodine species. In this paper, the performances of various commercial activated carbons towards the trapping of γ-labelled methyl iodide were evaluated in semi-pilot scale under different R.H. according to normalized procedures. A combination between the retention performances and the physico-chemical properties as deduced from several techniques was performed to gain insights about the AC influencing parameters on γ-CH_3I capture. Different trends were obtained depending on the impregnant nature and the studied conditions. A high sensitivity of KI/AC towards water vapor was outlined. At R.H. = 40%. The enhancement of water uptake by KI/AC as deduced from water adsorption experiments, leads to decrease the available microporosity for CH_3I physisorption, inducing therefore the reduction of performances as a function of KI content at these conditions. At R.H. = 90%, the adsorption mechanism was found to be governed by isotopic exchange reaction since 90% of the microporosity was occupied by water molecules. Therefore, a slight increase of DF was obtained in these conditions. This sensitivity was found to be of a lesser extent for TEDA/AC displaying the highest retention performances whatever the studied condition.

1. Introduction

As the rapid increase of the nuclear industry in the 21st century, the necessity to limit the release of radioactive substances into the environment remains a major challenge for the nuclear safety [1]. Among the most hazardous radionuclides, a particular attention is devoted to iodine radioactive species owing to the presence of volatile compounds (namely I_2 and CH_3I), their high mobility in environment and their specific affinity for the thyroid gland [2]. Methyl iodide (CH_3I) is resulted from reaction between I_2 and organic paints existing in the nuclear facilities [3][4].

Current filtration devices of the iodine trapping are classified into two categories [5]: wet processes using mainly scrubbing methods and dry processes through porous sorbents. Dry process is known to be more promising than wet methods, due to its high removal efficiency and low maintenance cost [5]. Depending on the context, different adsorbents are implemented at the industrial scale in order to prevent from the iodine dissemination to the environment. More particularly, activated carbons (AC) are widely used within the ventilation

networks of nuclear facilities to trap volatile iodine species in normal operating and degraded conditions [6]. The good performances of AC are assigned to their well-developed microporosity [7] (d pore < 2 nm) promoting therefore the capture of CH_3I by physisorption phenomena. However, the AC performances for CH_3I trapping are known to be drastically reduced under humid conditions due to the competitive adsorption between water vapor and methyl iodide [8]. The affinity of AC towards the CH_3I must be enhanced by impregnation with organic or inorganic compounds. The most used impregnants in the nuclear field [9] are triethylenediamine (TEDA, ≤ 5 wt.%) and potassium iodide (KI, 1 wt. %) interacting with CH_3I through different retention mechanisms [10][11][12][13]. On the one hand, TEDA is able to react with methyl iodide *via* different mechanisms of chemisorption depending on the R.H., resulting in the improvement of the adsorption performance of the AC [14]. On the other hand, the trapping mechanism of the radioactive CH_3I on KI impregnated AC is reported to involve an isotopic exchange reaction between the radioactive CH_3I and the stable KI. It is reported that the amount of the stable KI should be in excess in order to guarantee the efficient capture of radioactive CH_3I [15].

Despite the massive use of these adsorbents in the nuclear field, systematic studies of the intrinsic AC characteristics (textural properties, impregnants contents and speciation) towards γ-labelled methyl iodide retention are rarely investigated. The current investigations of the AC characteristics towards their adsorption performances remain generally at the laboratory scale through breakthrough curves or adsorption isotherms [16][17][18]. The existing publications based on the decontamination factor (DF) measurement following standardized procedures have rarely focused on the influence of the intrinsic properties of the adsorbent [19][20]. Nevertheless, recent studies of the AC performance are mainly focused on the TEDA impregnated AC with limited impregnation ratios, and no structure - activity correlation were determined [21]. Moreover, the lack of the attention for the KI impregnated AC and the associated performance comparisons with not-impregnated AC can also be noticed [12]. In that respect, the role played by KI as well as the correspondent mechanism are rarely focused in the literature.

In this study, we aimed therefore to gain insights on the most prominent factors towards the capture of radioactive methyl iodide in semi-pilot scale according to normalized procedures [22][23], by using different commercial formulations of activated carbons. In the first part, characterizations with different techniques (XPS, XRD, SEM-EDX, N_2 porosimetry…) are presented. In the second part, the decontamination factors towards γ-labelled methyl CH_3I deduced from the standardized norms are discussed depending on the water vapor content. The main objective was to establish relationships between the adsorbent parameters and its retention properties depending on the studied condition.

2. Experimental

2.1 Presentation of the tested adsorbents

Different formulations of commercial AC (grain size ranging from 2 to 3 mm) are used in this study. The studied materials derived from coco-nut shells were produced in the same batch in order to limit the dispersions in the AC characteristics. Different impregnation types of KI and TEDA were made but few details were provided regarding the exact synthesis protocol

as well as the precise impregnation ratio. On the one hand, co-impregnated AC (KI and TEDA) were tested with the aim to compare their properties with the *nuclear grade AC* currently used in the ventilation networks. On the other hand, the KI or TEDA impregnated AC were tested separately in order to better understand the effects due both molecules on the retention performances and the involved mechanisms depending on the studied conditions. The theoretical impregnation ratio of each AC is summarized in the Table 1.

Table 1 Summary of the theoretical impregnation ratio of different AC

KI impregnation (wt.%)	TEDA impregnation (wt.%)	Co-impregnation	
		KI (wt.%)	TEDA (wt.%)
0.1	1	0.5	1, 5, 10
0.5	3	1	1, 5, 10
1	5	2	1, 5, 10
2	7		
5	10		

2.2 Physicochemical characterizations

2.2.1 Chemical analysis

The experimental impregnant quantity (KI and TEDA) was determined using an extraction method [24]. Acetonitrile was used to extract the impregnants from batch experiments performed at ambient temperature. The amount of the extracted impregnants at equilibrium (overnight) was deduced from UV-Visible spectrophotometry (1900, Shimadzu). More particularly, absorbances at 247 nm and 225 nm were measured for KI and TEDA respectively using the Beer's Law.

Particular precautions were taken for the impregnants analysis. On the one hand, an excess of $Na_2S_2O_3$ was added during extraction in order to avoid the oxidation phenomena of iodine for KI impregnated AC. On the other hand, the subtraction of each molecule spectral contribution was required for co-impregnated materials due to KI and TEDA spectra interferences.

X-ray photoelectron spectroscopy (XPS) analysis were performed for some AC to gain insights on the chemical surface groups of the tested sorbents. Details about experimental acquisition and spectra deconvolution are reported in the supplementary (see S1, in ESI).

2.2.2 Textural properties

The porous structure of the investigated AC were derived from N_2 isotherms at 77 K (3FLEX, Micromeritics). Prior to each adsorption/desorption experiment, samples were preheated at 120°C overnight followed by an *in-situ* degassing at 120°C (10^{-6} mbar) for 12 h to remove most of the adsorbed impurities. Once the temperature was cooled down to 77 K, N_2 adsorption phase was started for increasing relative pressures (P/P_0) from 10^{-7} to 0.99. The desorption phase was then achieved for decreasing P/P_0 until 0.35. Specific surface areas (S_{BET}) were based on the BET calculation [25] and optimized by the Rouquerol's method [26]. The micropore volume and the micropore size distribution were deduced from the HK (Horwath-

Kawazoe) method for pore widths until 2 nm [27]. Finally, the total pore volume was measured from N_2 adsorption isotherms at relative pressure of 0.99 [28].

Additional information on the morphology of some AC were deduced from SEM/EDX characterizations. Details about the used instrument and the analysis conditions are reported in the supplementary (see S2, in ESI).

2.2.3 Water adsorption isotherms

H_2O adsorption isotherms were performed for some AC using a dynamic vapor sorption (DVS) Vacuum microbalance (Surface Measurement Systems, SMS). Prior to each sorption test, AC samples (mass = 60-70 mg) were outgassed at mild conditions (60 °C, 15 hours, vacuum of 10^{-5} Torr) to eliminate the residual humidity without inducing a significant modification of their surface chemistry according to recent works of Velasco et *al* [29]. Then, gravimetric measurements are carried out for R.H. ranging from 0% to 95% at 25°C. The thermodynamic equilibration for each tested R.H. was assumed when a water mass change of less than 0.0004 % per minute was obtained.

2.3 $CH_3{}^{131}I$ gas phase dynamic adsorption experiments

The retention of the $CH_3{}^{131}I$ was investigated within the PERSEE Facility [30], using a specific setup denoted as “low flow rates bench” (Fig. 1) to evaluate the performance of AC towards the capture of radioactive methyl iodide at semi-pilot scale. This experimental setup can be divided schematically into three main parts: (i) the generation of γ – labelled CH_3I and water vapor, (ii) the adsorbent to be tested (upstream stage) and (iii) the referenced AC (downstream stage) devoted to trap the fraction of methyl iodide not retained by the tested adsorbent. This adsorbent was the same for all the presented retention tests for comparison purposes.

Up to four AC can be tested simultaneously thanks to this test bench. Different sensors were placed in order to monitor the different test parameters, especially temperature, relative humidity and face velocity of the flowing gas. The experimental protocol developed for this setup was adapted from the ASTM3803 [22] and NFM62-206 standards [23] devoted to characterize the retention performances of commercial nuclear grade AC towards γ – labelled CH_3I.

The AC samples to be tested as well as the reference AC were prepared through the same geometry, according to a specific procedure summarized in the supplementary (see S3, in ESI). For all retention testes, a bed depth of 5 cm and bed density of 0.5 g/cm^3 were employed. Such conditions allow an AC loading in agreement with the normalized test procedures [22, 23].

Once the AC are prepared, a pre-equilibration under humidity (R.H. = 40% and 90% at 20°C) of at least 16h is made under flowing mode (gas flow rate of 17.5 L/min (NTP) corresponding to a face velocity of 25 cm/s and residence time of 0.2 s at 20°C) for both upstream and downstream sections. The objective is to achieve the equilibrium between the tested samples and the desired R.H. before the adsorption test. Then, the retention test was carried out using these same conditions. More particularly, a pulse (duration of 30 min) of γ-labelled CH_3I (C_0 = 0.15 ppmv) was generated from the following reaction:

$$(CH_3)_2SO_4 + 2NaI^* \rightleftharpoons 2CH_3I^* + Na_2SO_4$$

After 30 mins of the γ – labelled CH_3I generation, an elution phase of 60 min with air flow in the same conditions is carried out in order to take into account the desorption of physiosorbed CH_3I [23]. Finally, *ex-situ* γ-spectrometry measurements (*Cryo-Pulse 5 Plus, Canberra*) were carried out for both the upstream and downstream AC. DF can be therefore deduced from the following expression:

$$DF = \frac{A_{upstream} + A_{downstream}}{A_{downstream}}$$

Where $A_{upstream}$ and $A_{downstream}$ denote the measured ^{131}I activities by γ-spectrometry in the upstream and downstream stages (Figure 1) respectively. Due to the expected difference in the retention behavior as a function of the relative humidity, the injected activity of radioactive methyl iodide was adapted especially for moderately humid conditions, to increase the expected activity in the downstream section (generally close to the detection limit at R.H. = 40%). More precisely, initial ^{131}I activities per section equal to 62 and 617 KBq were targeted for R.H. of 40 and 90% respectively.

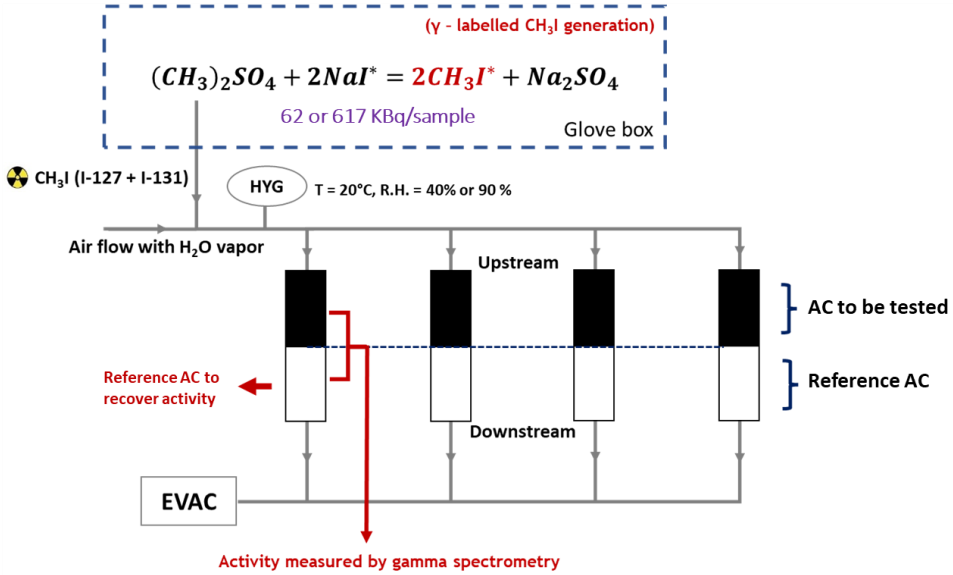

Figure 1 Schematic representation of the "low flow rates" test bench of PERSEE

3. Results and discussions

3.1 Physicochemical characterizations of impregnated AC

3.1.1. Chemical composition

The determined impregnant quantities of KI and TEDA are presented in the Figure 2 (a). Firstly, the absence of KI and TEDA molecules was checked for the not-impregnated AC. In addition, a quasi-linear relationship can be noticed when comparing experimental and theoretical contents. Nevertheless, a deviation of 23%, 15% and 27% from the theoretical amount was found for the tested TEDA, KI and co impregnated AC respectively (Figure 2 (a)). For example, contents of 0.69 wt. % and 3.85 wt. % were measured for KI and TEDA respectively for

theoretical contents of 1 wt. % (KI) and 5 wt. % (TEDA). These results were compared with CHNS analysis in some TEDA AC. The TEDA contents deduced form nitrogen quantity, were found to be close to the theoretical loadings despite some observed variabilities (Table S1). This discrepancy may be related to the presence of more bonded (*i.e.* chemisorbed) molecules that cannot be evidenced by the reported extraction method. Indeed, the molecular diameter of the acetonitrile (0.652 nm [31]) is found to be slightly higher than the expected pore width of the tested AC, indicating that the accessibility of the acetonitrile towards certain KI or TEDA sites may be hindered. These strongly bonded or inaccessible molecules can be nevertheless measured by CHNS technique based on a combustion step followed by chromatographic measurements. According to the further exchanges with the AC supplier, all the tested AC were impregnated using specific impregnation protocols [32] leading possibly to inaccessible fraction in TEDA and KI molecules using an acetonitrile extraction method. In the following parts, only theoretical contents will be presented since the deviation of experimental amounts from the indicated values was linear.

Additional information regarding the AC sample surface can be deduced from the XPS spectra presented in the Figure 2 (b). As expected, the considered samples are mainly carbonaceous (88-90 at. % in carbon) in agreement with the CHNS analysis (Table S1). Other elements resulting from the raw material and the further production steps can be also evidenced (Figure S1). We notice namely the presence of oxygen (8-10 at. %), nitrogen (0.5-2 at. %), potassium (0.2-1.1 at. %) and iodine (0.1-0.5 at. %). The semi-quantitative analysis using XPS gives also evidence for KI and TEDA impregnations by comparing the chemical composition of both starting and impregnated AC. An increase of the iodine surface contents has been observed without linear correlation for the tested materials. The discrepancy compared to the theoretical amount of KI is probably related to the XPS sensibility to AC surface (depth of about 1 nm) as comparison with the global characterizations by extraction and UV-Visible measurements. Moreover, potassium contents were analyzed in order to make sure from the stoichiometric K/I ratios. In the case of reference KI, a K/I ratio close of unity (~0.9) was found. However, a very large deviation from 1:1 stoichiometry was observed at the expense of iodine for 5%KI AC (K/I ~2), 1%KI5%TEDA (K/I ~5) and 2%KI5%TEDA AC (K/I~4). This discrepancy may be attributed to the presence of significant amount of potassium in the starting material (%K = 1.11 at. %, Figure S1), making it difficult to distinguish the native potassium (raw material) from additional potassium due to the KI impregnation. For TEDA, no correlation between the surface nitrogen concentrations with TEDA contents was possibly due to the volatility of this molecule under vacuum. Nevertheless, a quasi-similar amount of nitrogen (1.56 – 1.97 at. %) related to the strongly bonded TEDA species, was found for three adsorbents with 5 wt. % in TEDA as indicated in the Figure S1.

The deconvolution of XPS spectra allowed us to gain insights on the element speciation. It can be mentioned firstly that the tested AC display rather similar C1s (285 eV) and O1s (530 eV) speciation (Figure S2), in agreement with the use of the same batch and substrate for their production. On the one hand, the carbon speciation is mainly dominated by the sp^2 graphitic contribution (Figure S3) [33], consistently with the amorphous graphitic structures of these materials, as depicted from XRD characterizations (two broad peaks located at 22° and 43.5°, see Figure S4). Other contributions assigned to oxidized carbon species can also be identified

(alcohols, carbonyls, quinones, Figure S3). On the other hand, the O1s line is found to be composed of 5 contributions , consistent with the carbon oxidized species observed at the C1s line [34] (Figure S5).

Information about KI and TEDA speciation can be deduced from nitrogen and iodine peaks deconvolution. In the case of nitrogen (N1s), two peaks located at 398 eV (N1) and 400 eV (N2) are observed (Figure S6). The N1 peak corresponds to three-coordinated nitrogen N sigma-bonded to carbons (with sp^3 bonds), as in amines (N-H_3) and in TEDA (N-C_3) [35]. The N2 peak is rather associated with N-Csp^2 bonds, as for quaternary amines, that may be attributed to a nitrogen interaction with a carbon atom in the graphitic structure [36]. It is difficult to relate the TEDA quantity to the N1 speciation since N1 is already present on the not-impregnated AC and 5%KI AC. Then, the N1 speciation is not only contributed by the TEDA but also by other potential nitrogen functional groups on the AC surface. In general, it is observed that the speciation of the N1 and N2 remains the same for all the tested AC sample, indicating their similar surface characteristics. For iodine (I3d), two different components can be also displayed: 619 eV (I1) and 621 eV (I2) (Figure S7). The dominant contribution I1 is due to ionic I^- characteristic of the KI signature. While, the small one I2 is associated to less negative iodine ($I^{\delta-}$). A ratio between I1 and I2 of about 80/20 was found for all the tested samples, as a comparison with the reference KI product mostly made from the I1 peak (94%). The presence of the peak I2 for the tested AC sample may indicate the potential interaction of iodine with surface defects of the AC, leading to the formation of more covalent iodine species. The presence of this contribution may explain also the observed deviation from acetonitrile extraction, since the developed analytical method was only sensitive to I- component. Finally, a rather similar speciation of nitrogen and iodine can be observed when comparing the studied singly impregnated or co-impregnated AC. Therefore, it can be proposed that there is no interaction between TEDA and KI molecules within the AC. The absence of interaction could be explained by two factors: (i) different molecules localizations within the AC surface; (ii) a large excess of TEDA as a comparison with KI in the studied adsorbents (TEDA/KI molar ratios of 3.7 and 7.4 for 2%KI+5%TEDA and 1%KI+5%TEDA AC respectively).

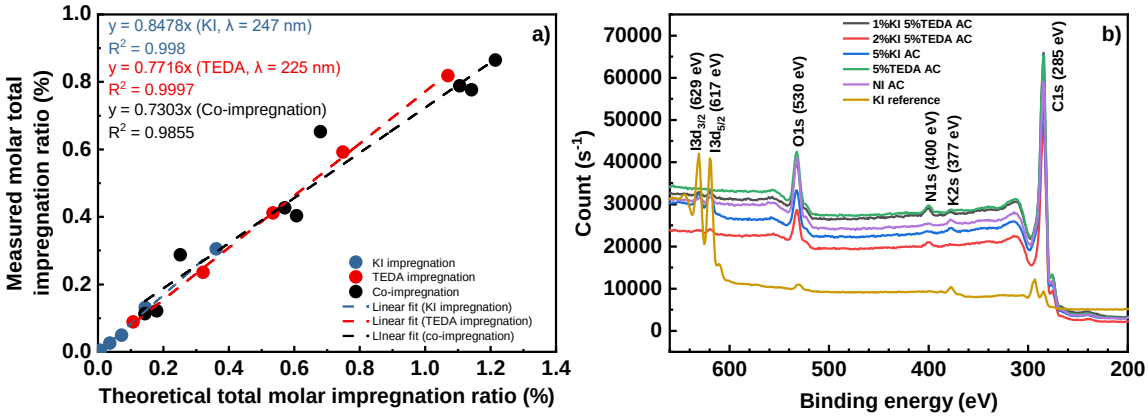

Figure 2 (a) Determined impregnation ratio; (b) XPS spectra for some of the tested AC

3.1.2. XRD and SEM/EDX analysis

Additional elements regarding KI and TEDA localizations within the investigated AC can be

deduced from XRD and SEM/EDX analysis. On the one hand, no new X-ray diffraction peaks typical of KI and TEDA lines were observed, indicating the absence of agglomeration of the impregnants on the external surface (Figure S4). Therefore, it can be proposed that these agents are well-dispersed within the internal porosity in molecular way. This observation was also confirmed by SEM/EDX investigations. Indeed, no substantial change before and after impregnation was noticed according to the different recorded SEM images. An example for the 2%KI and 5%TEDA AC is presented in the Figure 3 with increasing magnifications. More particularly, the 65000 magnification (Figure 3 (a)) reveals the presence of macropores presenting a typical geometry of the coconut shell based AC [21]. Other magnifications (Figures 3 (b) and (c)) show the existence of some particles heterogeneously distributed on the carbon surface. According to their EDX analysis, neither KI nor TEDA are identified. However, other elements can be depicted (such as magnesium, sodium, chlorine, silicon…) which are reported to be inherent to the raw material and the further fabrication steps [21]. Hence, KI and TEDA seem to be well dispersed within the internal porosity of the studied materials.

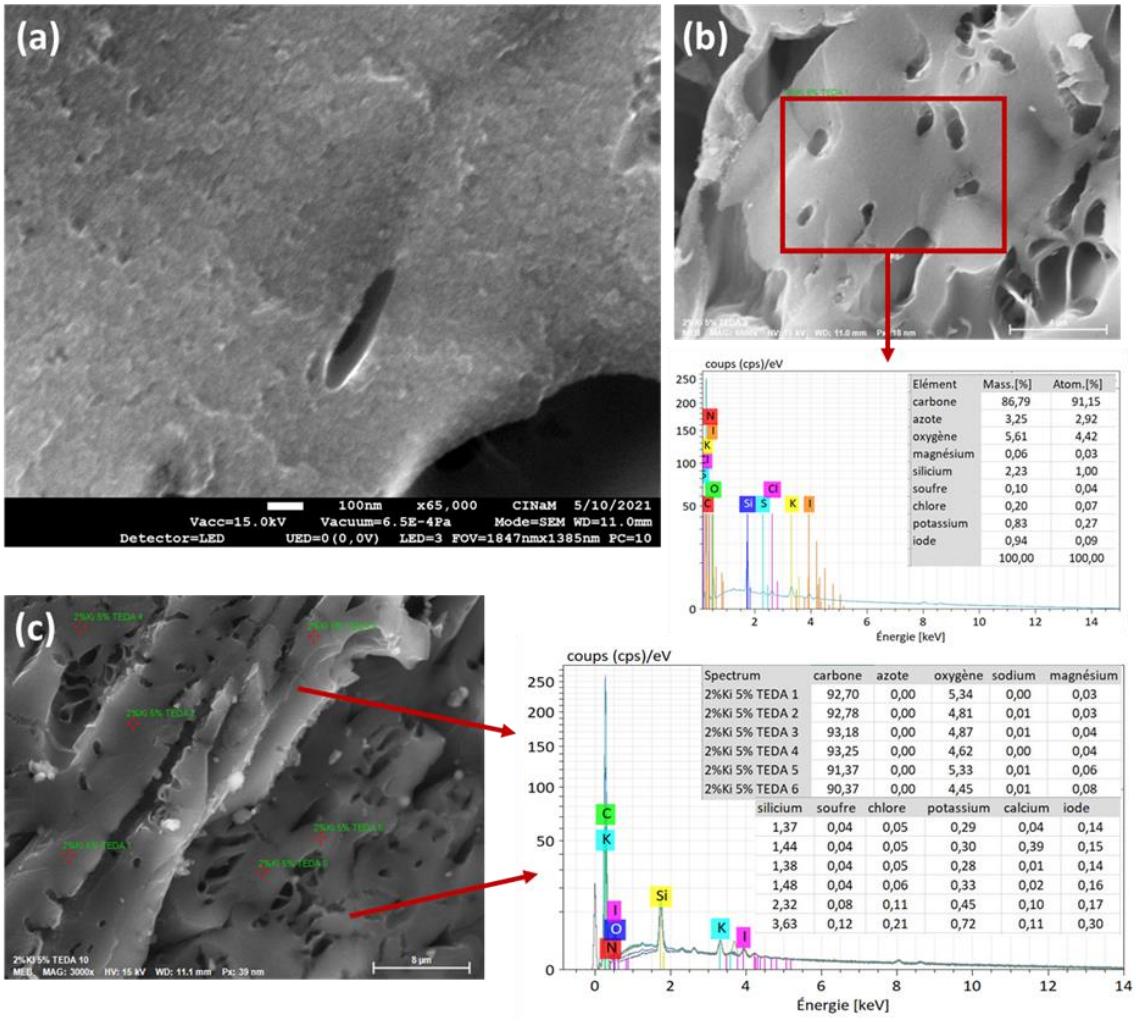

Figure 3 Selected SEM images of the 2%KI 5%TEDA AC: (a) magnification × 65000;(b) magnification × 6500 and EDX analysis in the rectangular area; (c) magnification × 3000 and EDX analysis at six locations

296 *3.1.3. Porous structure*

297 The effect of impregnants presence within the internal porosity of the tested AC is now
298 discussed in terms of porosimetric characteristics as deduced form N_2 adsorption/desorption
299 isotherms at 77 K. The obtained N_2 adsorption isotherms exhibit a type I, typical of
300 microporous materials [37] (Figure S8 in ESI). A very small hysteresis can be also depicted
301 indicating the presence of narrow mesopores [38], whose contribution was found to be
302 negligible (< 6 %). The associated porosimetric data (S_{BET} and V_{micro}) are summarized in the
303 Table 2. These parameters are expressed as average values from at least two measurements.
304 The related uncertainties are calculated using the standard error of the mean expressed at
305 coverage factor k=2 (*i.e*. confidence level of 95%). The tested AC exhibit in general high
306 specific surface area around 1000 m^2/g, with an important contribution due to the
307 microporous volume (V_{micro} / V_{pore} > 94%). The observed microporous characteristics of the
308 tested AC sample are in agreement with the AC made from coconut shell in the nuclear field.
309 This raw material is reported to be able to develop high microporosity for the AC [21][39].
310 Besides, the mean pore diameter deduced from the HK method is around 0.5 nm, making it
311 suitable for the CH_3I trapping (kinetic diameter of 0.5-0.6 nm [40]) by physisorption
312 phenomena.

313 The evolution of determined S_{BET} and V_{micro} as a function of the total molar impregnation ratio
314 is presented in the Figure 4. Two distinct zones can be depicted as function with the
315 impregnant content. For total molar impregnation lower than 0.4% (around 3 wt.% TEDA or
316 5 wt.% KI), a quasi-similar microporosity can be stated. Nevertheless, a closer look for low
317 impregnations contents (< 0.1 at. %) shows a slight increase of the S_{BET} and V_{micro} as a
318 comparison with the not impregnated AC. This unexpected increase is also reported in the
319 literature [41][42][43]. It can be postulated that a small amount of impregnation may create
320 more heterogeneity on the surface, inducing a slight overestimation of the microporosity. For
321 total molar impregnation ratio exceeding 0.4 %, a linear decreasing evolution can be observed
322 (Figure 4). For example, the S_{BET} decreases from 1097 m^2/g (3%TEDA, Table 2) until 715 m^2/g
323 (2% KI + 10% TEDA, Table 2). Indeed, the impregnation is known to induce partial blocking of
324 the porosity on the AC surface (especially the micropores)[44][45]. The observed
325 microporosity decrease may be assigned to the presence of KI and TEDA mainly within or in
326 the micropores openings. This observation seems to be in line with the previous XRD and
327 SEM/EDX analysis indicating the presence of such agents within the internal porosity without
328 agglomeration on the external surface. Moreover, the linear decrease of the textural
329 properties (S_{BET} and V_{micro}) as function of the global molar amount of impregnants, seems to
330 follow the same trend whatever the type of impregnation (TEDA, or co-impregnated). This
331 observed evolution is governed mainly by the TEDA contribution due to its large excess on
332 the detriment of KI (except for 2%KI+1%TEDA) for the studied co-impregnated AC. Such a
333 linear decreasing was also observed in the literature after TEDA impregnation [21][46][47].
334 This behavior was attributed to specific interaction between the nucleophile amine of TEDA
335 and π–electrons of the graphene [47][48].

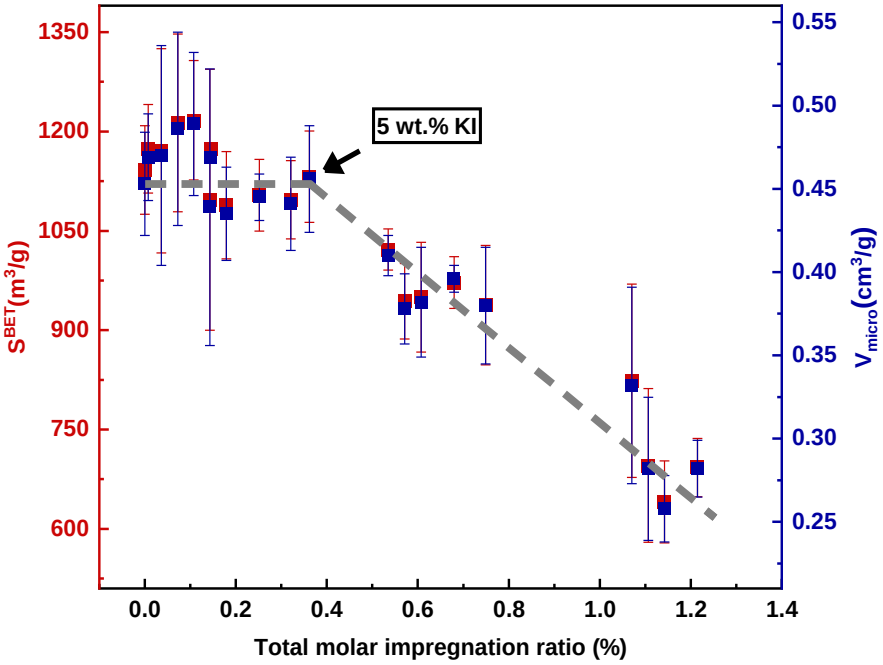

336

337 *Figure 4 Evolution of S_{BET} and V_{micro} towards total impregnation ratio*

338

339 *Table 2 Textural properties of the investigated AC from N_2 porosimetry*

Impregnation type	Total molar impregnation (%)	S_{BET} (m^2/g)	V_{micro} (cm^3/g)	d_{micro} (nm)	V_{pore} (cm^3/g)
NI	0.000	1142 ± 67	0.453 ± 0.031	0.473 ± 0.003	0.472 ± 0.032
0.1% KI	0.007	1174 ± 67	0.469 ± 0.026	0.474 ± 0.001	0.492 ± 0.030
0.5% KI	0.036	1171 ± 154	0.470 ± 0.066	0.480 ± 0.009	0.496 ± 0.075
1% KI	0.072	1213 ± 134	0.486 ± 0.058	0.482 ± 0.017	0.513 ± 0.061
1% TEDA	0.107	1217 ± 90	0.489 ± 0.043	0.485 ± 0.016	0.513 ± 0.051
0.5%KI + 1%TEDA	0.143	1097 ± 197	0.439 ± 0.083	0.478 ± 0.018	0.458 ± 0.086
2% KI	0.145	1174 ± 0	0.469 ± 0.002	0.479 ± 0.003	0.493 ± 0.003
1%KI + 1%TEDA	0.179	1089 ± 81	0.435 ± 0.028	0.479 ± 0.003	0.454 ± 0.029
2% KI + 1% TEDA	0.252	1104 ± 54	0.445 ± 0.014	0.487 ± 0.009	0.472 ± 0.011
3% TEDA	0.321	1097 ± 59	0.441 ± 0.028	0.488 ± 0.006	0.464 ± 0.029
5% KI	0.361	1132 ± 69	0.456 ± 0.032	0.484 ± 0.014	0.483 ± 0.034
5% TEDA	0.535	1022 ± 31	0.410 ± 0.012	0.492 ± 0.002	0.433 ± 0.009
0.5%KI + 5%TEDA	0.571	944 ± 57	0.378 ± 0.021	0.492 ± 0.012	0.394 ± 0.020
1%KI + 5%TEDA	0.607	950 ± 83	0.382 ± 0.033	0.492 ± 0.004	0.403 ± 0.035
2%KI + 5%TEDA	0.679	972 ± 39	0.396 ± 0.008	0.508 ± 0.020	0.420 ± 0.013
7% TEDA	0.749	938 ± 90	0.380 ± 0.035	0.501 ± 0.008	0.401 ± 0.035
10% TEDA	1.070	824 ± 146	0.332 ± 0.059	0.515 ± 0.003	0.343 ± 0.076
0.5%KI + 10%TEDA	1.106	696 ± 116	0.282 ± 0.043	0.518 ± 0.024	0.298 ± 0.014

1%KI + 10%TEDA	1.142	641 ± 62	0.258 ± 0.020	0.519 ± 0.010	0.268 ± 0.002
2%KI + 10%TEDA	1.214	693 ± 44	0.282 ± 0.017	0.526 ± 0.003	0.293 ± 0.003

340

341 3.2 γ-labelled CH_3I retention performances by impregnated activated carbons at semi pilot
342 scale

343 *3.2.1 Performances of co-impregnated AC*

344 The DF of the tested AC at RH = 40% and 90% were summarized in the Table 3 and shown in
345 the Figure 5. The reported DF are expressed as average values from at least 3 replicates. The
346 associated uncertainties are calculated using the standard error of the mean expressed at
347 coverage factor k=2. The co-impregnated AC exhibit separate retention performances
348 depending on the investigated condition. On the one hand, excellent filtering properties are
349 highlighted at RH = 40% with DF order of magnitude ranging from 10^4 to 10^5 (Table 3).
350 Therefore, the DF determined at this condition are found to be in agreement with the
351 required performances for AC currently implemented in the French nuclear industry [49]. A
352 closer look to the results displayed by co-impregnated materials indicates a different behavior
353 depending on the impregnation nature. Indeed, a decrease of DF values can be reported as a
354 function of KI content when fixing the TEDA quantity. For example, a reduction in
355 performances is noticed from (91958 ± 19879) to (12575 ± 2046) when varying KI contents
356 from 0.5 to 2 wt.% for a fixed TEDA quantity of 1 wt.% (Table 3). In contrast, progressive TEDA
357 impregnation from 1 to 5 wt.% (whatever the fixed loading of KI, Figure 5 (a)) contributes to
358 the enhancement of methyl iodide retention performances. For higher TEDA contents, a
359 rather similar DF is reported. Thus, it seems that the best retention performances at this
360 condition (T=20°C, RH = 40%) are obtained for the AC co-impregnated with 0.5 and 5 wt.% in
361 KI and TEDA respectively with a DF value of (173182 ± 4347). This composition seems to agree
362 well with the reported composition of nuclear grade activated carbons (%KI < 1 wt.%, TEDA
363 content of 5 wt.% [49]). Nevertheless, an uncertainty is still remaining concerning the role
364 played by KI in the removal of CH_3I through the tested methodology. In fact, higher DF value
365 was obtained without KI and for TEDA content of 5 wt.% (220228 ± 40203, Table 3).

366 On the other hand, a drastic decrease of DF for the studied co-impregnated AC is observed at
367 this second set of conditions, with corresponding DF around 1000 times lower than those
368 obtained at the previous conditions {T=20°C, RH = 40%}. This performances decrease is
369 consistent with the adverse effect related to the water vapor adsorption by AC [45]. The DF
370 of the tested co-impregnated AC are ranging from (31 ± 2.6) to (109 ± 25) in humid conditions.
371 As a comparison, a DF of about 100 is required for nuclear grade AC at this conditions, *i.e.* in
372 the presence of large excess of water vapor [49]. This order of magnitude is also reported in
373 several studies in the literature [19][21]. More particularly, a greater beneficial effect due to
374 TEDA impregnation as a comparison with KI can be observed. Indeed, TEDA contents of 5 or
375 10 wt.% are required to guarantee satisfactory retention performances towards CH_3I (DF
376 about 100, for KI content lower than 2 wt.%, Table 3). However, a negligible contribution due
377 to KI for CH_3I removal can be reported considering these tests. An even detrimental effect is
378 highlighted when increasing KI contents from 1 to 2 wt.% for fixed TEDA loadings of 5 or 10
379 wt.% (curves in red and blue, Figure 5 (b)). Indeed, the correspondent DF are only about (53
380 ± 14) and (60 ± 5.4) for (2%KI + 5%TEDA) AC and (2%KI + 10%TEDA) AC respectively (Table 3).

In addition, just a slight increase in DF performances was observed from (91 ± 6.5) to (106 ± 20) when increasing KI content from 0.5 to 1 wt.% and a for a fixed TEDA quantity of 5 wt.% (Table 3). For the other co-impregnated AC, quasi-similar DF values are reported when modifying the KI content (Table 3 and Figure 5 (b)). Considering the tested co-impregnated AC, the best retention performances are corresponding to 1 wt.% KI and 5 wt.% TEDA. The same impregnation combination is also reported for the commonly used nuclear grade AC [9]. This AC displays also a slightly higher performance than TEDA only impregnated AC (DF = 88 ± 15 for 5 wt.% TEDA, Table 3). Despite this enhancement, the contribution due to KI for CH_3I removal at this set of conditions is still negligible as a comparison with TEDA.

Overall, satisfying performances of the tested co-impregnated AC towards $CH_3{}^{131}I$ trapping are observed at different RH, with similar DF as the nuclear grade AC. Using this test methodology, the KI contribution may be masked because of the simultaneous presence of TEDA, presenting higher affinity for methyl iodide capture in moderately or highly humid conditions [44][46].

Therefore, the KI and TEDA impregnations will be separately investigated in the following parts. This will allow also us to better assess the role played by AC parameters towards their ability for radiotoxic CH_3I retention.

Table 3 Summary of DF for different AC at RH = 40% and 90%: T = 20°C, linear velocity = 25 cm/s, residence time = 0.2 s, initial 131I activity per AC = 62 KBq (RH = 90%) and 617 KBq (RH = 40%)

KI-impregnated AC			**TEDA-impregnated AC**		
KI%	DF (RH = 40%)	DF (RH = 90%)	TEDA%	DF (RH = 40%)	DF (RH = 90%)
0	10917 ± 4981	1.96 ± 0.08	1	106286 ± 35606	32 ± 5.8
0.1	6378 ± 1557	3.96 ± 0.98	3	210578 ± 62883	66 ± 2.4
0.5	3689 ± 1097	5.82 ± 0.61	5	220228 ± 46423	88 ± 15
1	2895 ± 769	7.33 ± 0.60	7	167621 ± 46755	103 ± 4.6
2	1587 ± 486	9.60 ± 1.32	10	128365 ± 32189	115 ± 5.9
5	236 ± 29	9.71 ± 0.87			
Co-impregnated AC					
KI%	TEDA%	DF (RH = 40%)		DF (RH = 90%)	
0.5	1	91958 ± 19879		33 ± 8.0	
0.5	5	173182 ± 43473		91 ± 6.5	
0.5	10	123006 ± 21794		100 ± 19	
1	1	37772 ± 10984		35 ± 5.0	
1	5	79281 ± 7743		106 ± 20	
1	10	86905 ± 23751		109 ± 25	
2	1	12575 ± 2046		31 ± 2.6	
2	5	49410 ± 11971		53 ± 14	
2	10	39445 ± 6884		60 ± 5.4	

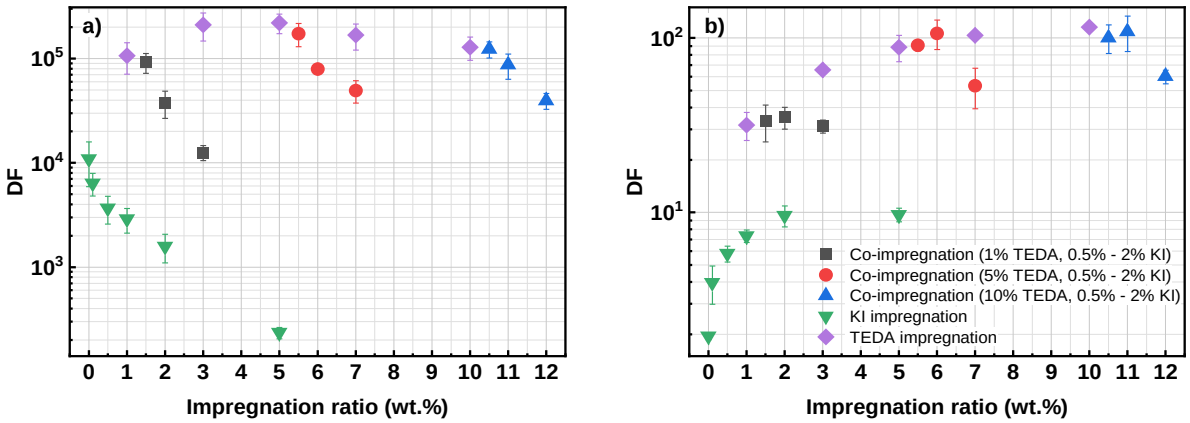

Figure 5 DF evolution for the tested AC towards the capture of γ-labelled CH_3I (T = 20°C, linear velocity = 25 cm/s, residence time = 0.2 s): a) RH = 40%, initial 131I activity per AC = 617 KBq; b) RH = 90%, initial 131I activity per AC = 62 KBq

3.2.2 Behavior of singly impregnated AC

3.2.2.1. T =20°C, RH = 40%

The specific behaviors of the impregnants are now discussed using singly impregnated AC. On the one hand, the TEDA impregnated AC present the highest DF among all the investigated adsorbents. Besides, similar DF evolution towards TEDA impregnation as the co-impregnated materials is observed (Figure 5 (a), curve in purple). Indeed, an enhancement of methyl iodide decontamination factors is observed from (106286 ± 35606) to (220228 ± 46423) for increasing TEDA contents from 1 to 5 wt.% (Table 3). For higher TEDA contents, a slight DF decrease is however observed until reaching a value of (128365 ± 32189) when TEDA amount is about 10 wt.% (Table 3).

On the other hand, the DF displayed by KI impregnated AC are found to be lower than that of the co-impregnated and TEDA impregnated AC (Table 3). More particularly, a paradoxical decrease of DF (Figure 5 (a), curve in green) is observed with the increase of KI content from (10917 ± 4981) for non-impregnated AC to only (236 ± 29) for 5 wt.% KI AC (Table 3). The obtained DF magnitude is in agreement with the literature under similar conditions [8][49]. This decreasing feature is also found to be consistent with the behavior displayed by co-impregnated AC when fixing the TEDA quantity, confirming the absence of any interaction between KI and TEDA molecules as observed in the previous chapter. Same orders of magnitude of DF for KI impregnated AC were also reported in the literature with RH ranging from 30% to 40% (T = 20 – 30°C) [8][50]. However, no attempt was performed before to better assess the role played by KI by comparing for instance with the non-impregnated AC.

3.2.2.2. T =20°C, RH = 90%

TEDA impregnated AC

An increasing relationship can be evidenced between DF and TEDA content until 7 wt.% (Figure 5 (b), curve in purple). More particularly, a DF increase from (32 ± 5.8) to (103 ± 4.6) can be highlighted for TEDA loadings of 1 wt.% and 7 wt.% respectively (Table 3). A less

pronounced increase in DF can be outlined for TEDA content of 10 wt.% (DF = (115 ± 5.9)). The observed DF are in the same order of magnitude of that reported in the literature under similar conditions for TEDA impregnated AC [8][20].

KI impregnated AC

Similar to the TEDA impregnated AC, the DF are also observed to increase with KI impregnation at {T=20°C, RH = 90%}, but with a less important extent. When varying KI content from 0 to 5 wt%, a slight increase of DF from (1.96 ± 0.08) to (9.71 ± 0.87) can be highlighted (Table 3 and Figure 5 (b), curve in green), indicating the inability of KI-impregnated AC to retain methyl iodide at the considered conditions compared to TEDA impregnation. Besides, the DF for a KI content of 2 wt.% and 5 wt.% are found to be similar ((9.60 ± 1.32) and (9.71 ± 0.87) respectively, Table 3), indicating a potential saturation of the AC performances for KI impregnation under current conditions. The inability of KI-impregnated AC to retain γ-labelled CH_3I seems to be consistent with the literature, where a magnitude of more than 600 of the DF decrease are outlined for RH ranging from 40 to 98% (residence time = 0.2 s) [8].

In general, singly impregnated AC present nearly the same DF evolutions as that of the co-impregnated AC. The absence of any interaction between TEDA and KI molecules can be therefore proposed, consistently with characterization results in the chapter II. An attempt to explain these observed trends will be presented in the next part.

3.2.2 Discussions about the role played by KI and TEDA

3.2.2.1 T = 20°C, RH = 40%

In order to explain the obtained DF evolutions (Figure 5), it is necessary to evaluate all the potential involved mechanisms. More precisely, three mechanisms are distinguished: the physisorption phenomena (controlled by the microporosity and the micropore filling of H_2O), the chemisorption *via* TEDA and the isotopic exchange reaction due to KI impregnation. Under moderately humid conditions (T = 20°C, RH = 40%), the physisorption mechanism was generally reported to be dominant compared to chemisorption phenomena or the potential isotopic exchange [46]. Therefore, a specific attention is devoted to assess the influencing parameters towards physisorption in this first set of condition.

On the one hand, the microporosity of the KI and TEDA impregnated AC present different features depending on the impregnation ratio. According to the previous characterization of the porous structure, the decreasing evolution of the microporosity cannot be observed for low impregnation ratio (< 0.4 % in molar, Figure 4), which corresponds to the studied KI impregnated AC and 3% TEDA AC (Table 2). In contrast, a more significant reduction in the microporosity was obtained for other TEDA AC because of a higher impregnation molar ratio (up to 10 wt.% corresponding to molar fraction of 1.07 %). The extent of the reduction in microporosity can reach more particularly about 27 % for a TEDA content of 10 wt.% (Table 2). To sum-up, the starting microporosity (*i.e.* before the pre-equilibration step) can be considered to be similar for KI impregnated AC but decreasing for TEDA impregnated AC especially after 3 wt.% in TEDA.

On the other hand, the available microporosity for CH_3I trapping can be influenced by the pre-adsorbed H_2O during the pre-equilibration step performed before retention test. Therefore, H_2O adsorption isotherms were determined at T=25°C for the studied singly-impregnated AC. The obtained curves are presented in the supplementary (see Figures S9 and S10). The obtained isotherms are of type V according to IUPAC classifications [51]. In the low-pressure range, adsorbent/adsorbate interactions are weak due to the hydrophobic character of AC surface. At Higher relative humidity, the water uptake is mainly controlled by the AC microporosity due to the micropore filling phenomena [52][53].

For this first studied condition (T=20°C, RH = 40%), the attention was focused on the water uptake at 30 and 95% (T =25°C). The correspondent results for different AC are reported in the Table 4. Different behaviors can be highlighted depending on the investigated impregnant. On the one hand, a significant increase of the adsorbed amount of H_2O was observed with KI impregnation (Figure 6 (a)). For example, an increase of water uptake from about 15 $mg \cdot g^{-1}$ to about 56 $mg \cdot g^{-1}$ was obtained when moving from non-impregnated AC to 5%KI AC (Table 4). Indeed, KI molecules may play primary clustering or nucleation sites towards water vapor adsorption at low RH, allowing therefore to reduce the hydrophobic character of AC [44][53]. On the other hand, the adsorbed amount of H_2O using the same conditions {T=25°C, RH = 30%} seems to be quasi-similar for the different tested TEDA AC (Figure 6 (a)), indicating a less effect due to nucleation for TEDA as a comparison with KI. Moreover, a lower water uptake was generally obtained for TEDA impregnated materials (a value ranging from 29 to 35 $mg \cdot g^{-1}$, Table 4).

Table 4 Summary of the adsorbed amount of H_2O at 25°C for different AC for DF at (T = 20°C, RH =

40%)

Impregnation	V_{micro} (cm^3/g)	Adsorbed H_2O at RH = 30%* (mg/g)	Adsorbed H_2O at RH = 95% (mg/g)	H_2O filling fraction at RH = 30% (%)	Available V_{micro} (cm^3/g)	DF
Non impregnated	0.453	15.4	397.4	4	0.435	10917
0.1 wt.% KI	0.469	29.7	364.8	8	0.431	6378
0.5 wt.% KI	0.470	33.4	343.1	10	0.424	3689
1 wt.% KI	0.486	44.4	353.9	13	0.425	2895
2 wt.% KI	0.469	38.6	385.4	10	0.422	1587
5 wt.% KI	0.456	56.1	342.4	16	0.381	236
3 wt.% TEDA	0.441	34.1	320.4	11	0.394	210578
5 wt.% TEDA	0.410	34.8	364.3	10	0.371	220228
7 wt.% TEDA	0.380	33.1	329.5	10	0.342	167621
10 wt.% TEDA	0.332	28.9	342.4	8	0.304	128365

* The conditions of the adsorption isotherms of H_2O (T=25°C, RH = 30%) are equivalent to the conditions of the retention test (T=20°C, RH = 40%) in terms of absolute humidity.

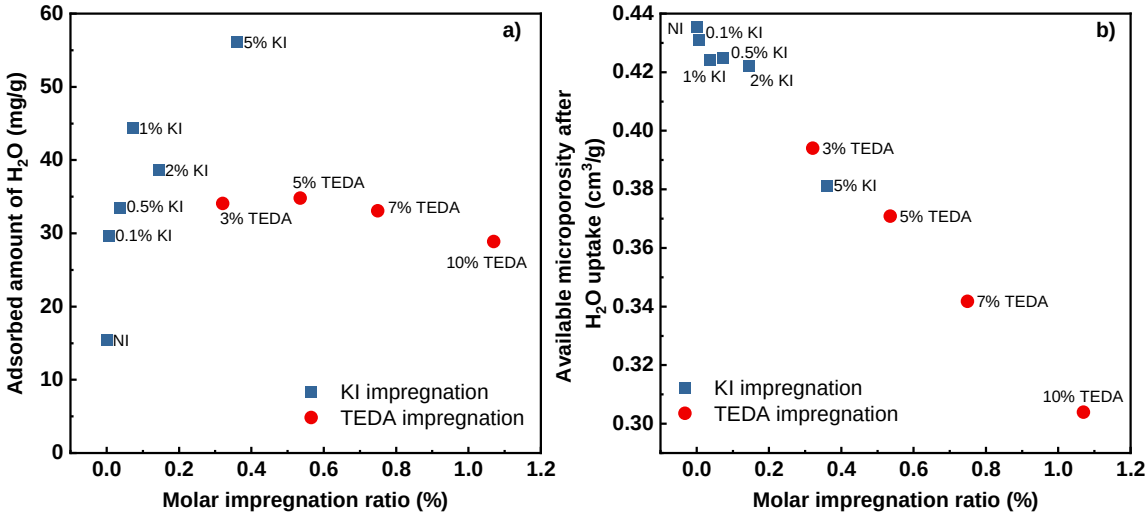

Figure 6 a) Pre-adsorbed H_2O versus the molar impregnation ratio at T = 25°C, RH = 30%; b) Available microporous volume after water uptake at T= 25°C, RH = 30% versus molar impregnation ratio

Regarding these considerations, it is necessary to determine the available microporous volume by multiplying the starting V_{micro} (as deduced from HK model) and the fraction of residual pores (1-H_2O filling fraction). As depicted in the Figure 6 (b), the available microporosity after water uptake decreases for both KI and TEDA impregnation. This reduction is attributed to different reasons depending on the molecule nature. For KI, this decrease is related to the enhancement of adsorbed H_2O at low RH after KI progressive loading. For TEDA, this trend is assigned to the decrease of microporosity because of the presence of TEDA within or in the openings of AC pores (Table 2). Therefore, the contribution of physisorption in all cases is expected to decrease after KI and TEDA impregnation.

For TEDA impregnated AC, the contribution of the physisorption is proved to be decreased. In the meantime, the contribution of the chemisorption is expected to increase with TEDA content. More precisely, the reactivity of TEDA at such moderately humid conditions {T = 20°C, RH = 40%} is reported to be dominated by an alkylation mechanism based on CH_3I dissociation followed by the formation of stable ammonium [48]. Hence, The DF evolution for TEDA impregnation at RH = 40% can be considered as a compromise between these two opposite mechanisms. According to the obtained results, the optimum TEDA impregnation corresponding to these two mechanisms seems to be 5 wt.%, where the accessible microporosity is decreased only by 15% against 23% with 7wt.% of TEDA, for instance.

It is reasonable to think that the DF evolution for KI impregnated AC at the studied conditions should be the same as displayed by TEDA impregnated AC. Indeed, there are also two mechanisms that work oppositely with KI content: the physisorption and the isotopic exchange led by the KI. However, it seems that the DF evolution for KI AC at {T = 20°C, RH = 40%} is dominated by physisorption and more particularly by the pre-adsorbed amount of water vapor during the equilibration step. This unusual observation is evidenced in the Figure 7 which shows the increasing evolution of DF versus the available microporosity for $CH_3{}^{131}I$ retention. Finally, it can be proposed that the trapping performance of the γ–labelled CH_3I for KI impregnated AC at moderately humid conditions is only dominated by the physisorption influenced itself by the water pre-adsorption. Therefore, this trend may indicate in other words the absence of the isotopic exchange under the first set of conditions.

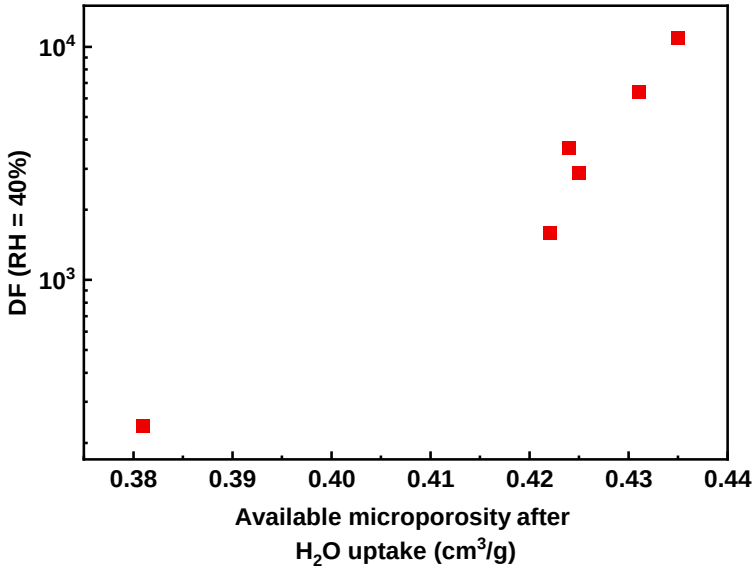

Figure 7 DF evolution (logarithmic scale) versus the available microporosity for KI impregnated AC (RH = 40%)

The role played by TEDA and KI towards the capture of CH_3I under more humid conditions will be discussed in the next section.

3.2.2.2 T = 20°C, RH = 90%

In these conditions, the significant changes in DF evolution compared to RH = 40% indicates the change of each trapping mechanism contribution (physisorption, chemisorption and the isotopic exchange). Using the same strategy, the physisorption contribution can be firstly

investigated using the adsorption isotherms of H_2O (T=25°C, Figures S9 et S10). As summarized in the Table 5, all the tested AC present significant amount of pre-adsorbed H_2O regardless the impregnation type (adsorbed amount higher than 300 $mg \cdot g^{-1}$). The water molecules are reported to be firstly adsorbed on the AC surface due to the strong chemisorption of the water molecules with functional groups as mentioned in the previous section [54][55]. Then, water clusters are progressively formed on the AC surface through the formation of hydrogen bonds [54][55], corresponding to the micropore filling of the water molecules. The increase of the pre-adsorbed amount of H_2O compared to RH = 40% induces a huge increase of the micropore filling fraction to about 90% (Table 5), indicating a strong competitive adsorption between CH_3I and H_2O. Consequently, the deduced available microporous volume for the impregnated AC is found to be less than 0.08 $cm^3 \cdot g^{-1}$ (Figure 8), which is almost negligible compared to the first set of conditions. To sum up, it can be concluded that the contribution of the physisorption is significantly reduced at RH = 90% since the accessibility to the active sites for physisorption is largely hindered by H_2O [10]. The significant reduction of the physisorption for all the tested AC under current conditions explains the drastic diminution of DF compared to RH = 40%.

Apart from the significant decrease of DF at RH = 90% compared to RH = 40%, the DF were found to increase with both TEDA and KI impregnations (Figure 5), which is clearly assigned to the chemisorption and the isotopic exchange respectively, since there is no other mechanism responsible for such increase of the AC performance in these conditions. Taking into account the low available microporosity that still remains at RH = 90%, it can also be proposed that as a preliminary step for the adsorption phenomena [15][56], the physisorption is no longer dominant for the CH_3I removal under current conditions. Nevertheless, the extent of DF increase due to the KI impregnation is less important as a comparison with TEDA, which is due to its high reactivity. Unlike the CH_3I dissociation mechanism for TEDA at RH = 40%, a protonation mechanism between CH_3I, H_2O and TEDA results to the formation of a molecular complex of TEDA/CH_3I under humid conditions, enhancing the chemical interaction of TEDA with CH_3I [46][47]. Besides, the saturation of the DF increase between 2 wt.% and 5 wt.% in KI may be assigned to the increase of the diffusion resistance by pre-adsorbed H_2O and deposited KI [46].

Table 5 Summary of the adsorbed amount of H_2O at 25°C for different AC for DF at (T = 20°C, RH =

576 *90%)*

Impregnation	V_{micro} (cm^3/g)	Adsorbed H_2O at RH = 70%* (mg/g)	Adsorbed H_2O at RH = 95% (mg/g)	H_2O filling fraction at RH = 70% (%)	Available V_{micro} (cm^3/g)	DF
Non impregnated	0.453	305.0	397.4	77	0.11	2.0
0.1 wt.% KI	0.469	304.7	364.8	84	0.08	4.0
0.5 wt.% KI	0.470	300.9	343.1	88	0.06	5.8
1 wt.% KI	0.486	317.8	353.9	90	0.05	7.3
2 wt.% KI	0.469	328.4	385.4	85	0.07	9.6
5 wt.% KI	0.456	317.4	342.4	93	0.03	9.7
3 wt.% TEDA	0.441	281.3	320.4	88	0.05	66
5 wt.% TEDA	0.410	298.0	364.3	82	0.07	88
7 wt.% TEDA	0.380	278.7	329.5	85	0.06	103
10 wt.% TEDA	0.332	285.4	342.4	83	0.06	115

577 * The conditions of the adsorption isotherms of H_2O (T = 25°C, RH = 70%) are equivalent to the conditions of the
578 retention test (T = 20°C, RH = 90%) in terms of absolute humidity.
579

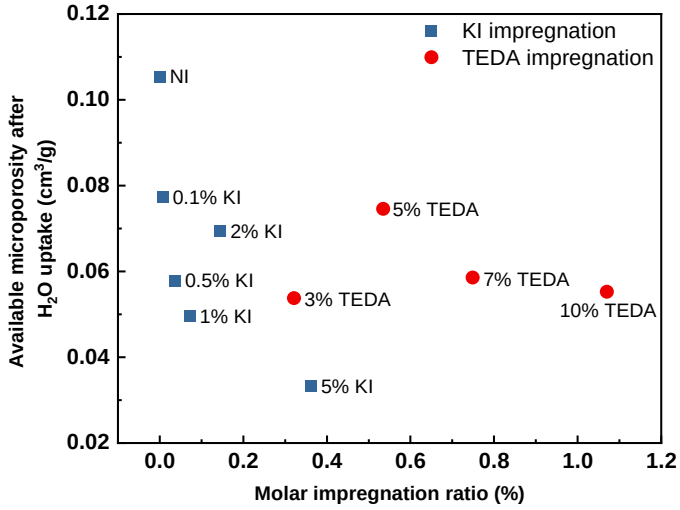

580

581 *Figure 8 Available microporous volume after water uptake at T = 25°C, RH = 70% versus molar*
582 *impregnation ratio*

583 It can be noticed that the isotopic exchange *via* KI seems to be observed only under humid
584 conditions. Similar tendencies were reported in the literature using the breakthrough curves
585 measurements for 5%KI_3 impregnated AC (equal amount of KI and I_2) [57]. Despite the
586 different experimental conditions (4625 Bq/m^3 of $CH_3{}^{131}I$, RH = 86%), it is observed that the
587 penetration of radioactive CH_3I is less than that of stable CH_3I, which justifies the presence of
588 the isotopic exchange during the fix-bed adsorption experiment [57]. More particularly, the
589 effect of the isotopic exchange becomes more significant during the breakthrough phase, and
590 no specific effect was observed at the beginning of the breakthrough curve (retention phase).

Hence, it is assumed that the effect of the isotopic exchange can only be observed when the KI impregnated AC are in the breakthrough phase. At RH = 40% in the current study, the conversion of DF to trapping efficiency indicates that the tested KI impregnated AC are still in the retention phase. However, the low value of DF at RH = 90% indicates the breakthrough of the AC. Hence, the effect of the isotopic exchange was only observed at RH = 90%. Nevertheless, a slight contribution from this mechanism can be highlighted using the normalized protocol test.

4. Conclusion

In this paper, the behaviors of KI and/or TEDA impregnated AC towards the capture of $CH_3{}^{131}I$ are investigated at different RH. First, a characterization of chemical, textural and structural properties of the investigated AC was performed. The presence of KI or TEDA has been evidenced for all the tested AC, but a slight and linear difference was observed between the theoretical and the experimental content of such molecules. SEM/EDX and XRD characterizations for some AC have shown that these entities are well dispersed within the internal porosity without clusters formation on the external surface of the tested materials. The absence of any interaction between KI and TEDA is further confirmed by the DF evolution for the co-impregnated AC, as they share similar tendencies with the singly impregnated AC. The tested AC present similar carbon and oxygen speciation as deduced from XPS, confirming the similar surface characteristics of these carbonaceous materials derived from the coconut shells produced in the same batch. Insights about the nitrogen and iodine speciation regarding the TEDA and KI impregnation, were also presented. The investigated AC are found to be essentially microporous (> 94 %), in agreement with AC produced from coconut shells. In addition, both the S_{BET} and V_{micro} decrease with the total impregnation due to the partial blocking of the AC porosity (especially the micropores) induced by the presence of TEDA and KI species within the internal porosity. A such micropore blockage becomes more significant for total molar impregnation ratio exceeding 0.4% (3 wt. % TEDA and 5 wt.% KI).

The investigation of $CH_3{}^{131}I$ adsorption behavior at RH = 40% and 90% revealed different features. At RH = 40%, all the tested AC exhibit good performance of $CH_3{}^{131}I$ trapping, with a DF up to 2.2×10^5. More particularly, it is observed that the DF decreases paradoxically with KI impregnation where the isotopic exchange was found to be absent. This decrease is due to the increased amount of the adsorbed H_2O results from the nucleation effect of KI impregnation, leading to the diminution of the available microporosity for physisorption. On the contrary, the DF evolution for TEDA at RH = 40% is found to be a compromise between the diminution of the available microporosity and the increase of the chemisorption *via* TEDA, with an optimal TEDA impregnation at 5 wt.%. At RH = 90%, a drastic decrease of DF is observed for all the AC, with DF about 1000 times lower than that at RH = 40%. The optimal impregnation at RH = 90% is obtained with 1% KI and 5% TEDA, in agreement with the composition of the nuclear grade activated carbons. The increase of the DF with TEDA and KI at RH = 90% was found to be directly related to the chemisorption and the isotopic exchange respectively. The extent of the DF increase when using TEDA was found to be more important as a comparison with KI, thanks to its higher reactivity CH_3I under different conditions.

Furthermore, the effect of the isotopic exchange led by KI was slightly and only observed through adsorption experiments at RH = 90%, by assuming its occurrence under breakthrough phase in agreement with literature studies.

In these works, different parameters of the AC towards their ability for radiotoxic CH_3I retention under semi pilot scale have been evaluated. Additional investigation of the AC performances will be further conducted under lab scale. The main objective is to elucidate the importance of the isotopic exchange by measuring the breakthrough curves of both $CH_3{}^{131}I$ and $CH_3{}^{127}I$ for KI impregnated AC. The roles of AC parameters towards the isotopic exchange will also be evaluated.

5. Acknowledgements

The authors would like to thank Denys Grekov from the IMT-Atlantique for performing CHNS analysis on some activated carbons. The research leading to these results is partly funded by the Institut de Radioprotection et de Sûreté Nucléaire (IRSN). This work was performed within the "Iodine" research program of the IRSN.

6. References

[1] E. Bertel and P. Wilmer, "Nuclear energy in a sustainable development perspective," *Organ. Econ. Coop. Dev. Energy Agency Paris, Fr.*, 2000.

[2] B. Clément *et al.*, "State of the art report on iodine chemistry," *NEA/CSNI/R(2007)1*, 2007.

[3] D. Haefner, T. Tranter, "Methods of gas phase capture of iodine from fuel reprocessing off-gas: a literature survey," *Idaho Natl. Lab.*, 2007.

[4] L. Bosland, S. Dickinson, G.A. Glowa, L.E. Herranz, H.C. Kim, D.A. Powers, M. Salay, S. Tietze, , "Iodine–paint interactions during nuclear reactor severe accidents," *Ann. Nucl. Energy*, vol. 74, pp. 184–199, 2014.

[5] S. U. Nandanwar, K. Coldsnow, V. Utgikar, P. Sabharwall, and D. E. Aston, "Capture of harmful radioactive contaminants from off-gas stream using porous solid sorbents for clean environment–A review," *Chem. Eng. J.*, vol. 306, pp. 369–381, 2016.

[6] R. T. Jubin, *A literature survey of methods to remove iodine from off-gas streams using solid sorbents*. Citeseer, 1979.

[7] C. Y. Yin, M. K. Aroua, and W. M. A. W. Daud, "Review of modifications of activated carbon for enhancing contaminant uptakes from aqueous solutions," *Sep. Purif. Technol.*, vol. 52, no. 3, pp. 403–415, 2007.

[8] C. M. Ecob, A. J. Clements, P. Flaherty, J. G. Griffiths, D. Nacapricha, and C. G. Taylor, "Effect of humidity on the trapping of radioiodine by impregnated carbons," *Sci. Total Environ.*, vol. 130–131, no. C, pp. 419–427, 1993.

[9] B. Collinson, L. R. Taylor, and P. Meddings, "Trapping performance of 1.5% KI 207B charcoal for methyl iodine in CO_2 at high temperature and pressure," in *Proceedings of the 20th DOE/NRC nuclear air cleaning conference. Sessions 1--5*, 1989, pp. 537–559.

[10] J. Huve, A. Ryzhikov, H. Nouali, V. Lalia, G. Augé, and T. J. Daou, “Porous sorbents for the capture of radioactive iodine compounds: a review,” *RSC Adv.*, vol. 8, no. 51, pp. 29248–29273, 2018.

[11] V. R. Deitz, “Interaction of radioactive iodine gaseous species with nuclear-grade activated carbons,” *Carbon N. Y.*, vol. 25, no. 1, pp. 31–38, 1987.

[12] J. Zhou, S. Hao, L. Gao, and Y. Zhang, “Study on adsorption performance of coal based activated carbon to radioactive iodine and stable iodine,” *Ann. Nucl. Energy*, vol. 72, pp. 237–241, 2014, doi: 10.1016/j.anucene.2014.05.028.

[13] Y. S. Kim, “Study on adsorption characteristics and deterioration patterns of an impregnated active carbon under a simulated service condition of the filtering system at a nuclear power plant,” 1989.

[14] E. Aneheim, D. Bernin, and M. R. S. J. Foreman, “Affinity of charcoals for different forms of radioactive organic iodine,” *Nucl. Eng. Des.*, vol. 328, pp. 228–240, 2018.

[15] J. L. Kovach, “History of radioiodine control,” in *Proceedings of 25th DOE/NRC Nuclear Air Cleaning and Treatment Conference*, 1998, pp. 304–319.

[16] H.-K. Lee and G.-I. Park, “Adsorption characteristics of elemental iodine and methyl iodide on base and TEDA impregnated carbon,” *Nucl. Eng. Technol.*, vol. 28, no. 1, pp. 44–55, 1996.

[17] G.-I. Park, I.-T. Kim, J.-K. Lee, S.-K. Ryu, and J.-H. Kim, “Effect of Temperature on the Adsorption and Desorption Characteristics of Methyl Iodide over TEDA-Impregnated Activated Carbon,” *Carbon Lett.*, vol. 2, no. 1, pp. 9–14, 2001.

[18] L. Tong, T. Yue, P. Zuo, X. Zhang, C. Wang, J. Gao, K. Wang, “Effect of characteristics of KI-impregnated activated carbon and flue gas components on Hg0 removal,” *Fuel*, vol. 197, pp. 1–7, 2017, doi: 10.1016/j.fuel.2016.12.083.

[19] H. C. Lee, D. Y. Lee, H. S. Kim, and C. R. Kim, “Performance evaluation of TEDA impregnated activated carbon under long term operation simulated NPP operating condition,” *Nucl. Eng. Technol.*, vol. 52, no. 11, pp. 2652–2659, 2020.

[20] B.-S. Choi, S.-B. Kim, J. Moon, and B.-K. Seo, “Evaluation of decontamination factor of radioactive methyl iodide on activated carbons at high humid conditions,” *Nucl. Eng. Technol.*, vol. 53, no. 5, pp. 1519–1523, 2021.

[21] C. M. González-García, J. F. González, and S. Román, “Removal efficiency of radioactive methyl iodide on TEDA-impregnated activated carbons,” *Fuel Process. Technol.*, vol. 92, no. 2, pp. 247–252, 2011.

[22] “ASTM D3803-91(2014), Standard Test Method for Nuclear-Grade Activated Carbon,” 2014.

[23] “NF M62-206, Méthode de contrôle du coefficient d’épuration des pièges à iode,” 1984.

[24] Y. S. Aim, “Ultraviolet spectrometric method of analyzing chemical impregnants of a nuclear grade active carbon and its applications for managing the carbon filter at a nuclear regulatory laboratory and plants,” in *Proceedings of the 19th DOE/NRC Nuclear*

Air Cleaning Conference, 1987, pp. 221–236.

[25] S. Brunauer, P. H. Emmett, and E. Teller, "Adsorption of gases in multimolecular layers," *J. Am. Chem. Soc.*, vol. 60, no. 2, pp. 309–319, 1938.

[26] J. Rouquerol, P. Llewellyn, and F. Rouquerol, "Is the BET equation applicable to microporous adsorbents," *Stud. Surf. Sci. Catal*, vol. 160, no. 07, pp. 49–56, 2007.

[27] G. Horváth and K. Kawazoe, "Method for the calculation of effective pore size distribution in molecular sieve carbon," *J. Chem. Eng. Japan*, vol. 16, no. 6, pp. 470–475, 1983.

[28] B. Sellergren and A. J. Hall, "Fundamental aspects on the synthesis and characterisation of imprinted network polymers," in *Techniques and Instrumentation in Analytical Chemistry*, vol. 23, Elsevier, 2001, pp. 21–57.

[29] L. F. Velasco, D. Snoeck, A. Mignon, L. Misseeuw, C.O. Ania, S. Van Vlierberghe, P. Dubruel, N. de Belie, P. Lodewyckx, "Role of the surface chemistry of the adsorbent on the initialization step of the water sorption process," *Carbon N. Y.*, vol. 106, pp. 284–288, 2016.

[30] M. Chebbi, B. Azambre, C. Monsanglant-Louvet, B. Marcillaud, A. Roynette, and L. Cantrel, "Effects of water vapour and temperature on the retention of radiotoxic CH_3I by silver faujasite zeolites," *J. Hazard. Mater.*, p. 124947, 2020.

[31] S. C. Lee, S.Y. Kim, W.S. Lee, S.Y. Jung, B.W. Hwang, D. Ragupathy, D.D. Lee, S.Y. Lee, J.C. Kim,"Effects of textural properties on the response of a SnO_2-based gas sensor for the detection of chemical warfare agents," *Sensors*, vol. 11, no. 7, pp. 6893–6904, 2011.

[32] S.-G. Ro and H.-K. Lee, "Method and apparatus for manufacturing TEDA-impregnated active carbon in fluidized bed type absorbing tower by generating TEDA vapor by means of hot air." Google Patents, Aug. 11, 1998.

[33] H. Estrade-Szwarckopf, "XPS photoemission in carbonaceous materials: A 'defect' peak beside the graphitic asymmetric peak," *Carbon N. Y.*, vol. 42, no. 8–9, pp. 1713–1721, 2004.

[34] M. E. Schuster, M. Havecker, R. Arrigo, R. Blume, M. Knauer, N.P. Ivleva, D.S. Su, R. Niessner, R. Schlogl,"Surface sensitive study to determine the reactivity of soot with the focus on the European emission standards IV and VI," *J. Phys. Chem. A*, vol. 115, no. 12, pp. 2568–2580, 2011.

[35] Y. Hayashi, G. Yu, M.M. Rahman, K.M. Krishna, T. Soga, T. Jimbo, M. Umeno, "Spectroscopic properties of nitrogen doped hydrogenated amorphous carbon films grown by radio frequency plasma-enhanced chemical vapor deposition," *J. Appl. Phys.*, vol. 89, no. 12, pp. 7924–7931, 2001.

[36] J. T. Titantah and D. Lamoen, "Carbon and nitrogen 1s energy levels in amorphous carbon nitride systems: XPS interpretation using first-principles," *Diam. Relat. Mater.*, vol. 16, no. 3, pp. 581–588, 2007.

[37] S. Brunauer, L. S. Deming, W. E. Deming, and E. Teller, "On a theory of the van der Waals adsorption of gases," *J. Am. Chem. Soc.*, vol. 62, no. 7, pp. 1723–1732, 1940.

[38] F. R. Ribeiro and M. Guisnet, *Les zéolithes, un nanomonde au service de la catalyse*. EDP sciences, 2006.

[39] C. G. Doll, C.M. Sorensen, T.W. Bowyer, J.I. Friese, J.C. Hayes, E. Hoffmann, R. Kephart, "Abatement of xenon and iodine emissions from medical isotope production facilities," *J. Environ. Radioact.*, vol. 130, pp. 33–43, 2014.

[40] B. S. Choi, G. Il Park, J. H. Kim, J. W. Lee, and S. K. Ryu, "Adsorption equilibrium and dynamics of methyl iodide in a silver ion-exchanged zeolite column at high temperatures," *Adsorption*, vol. 7, no. 2, pp. 91–103, 2001.

[41] J. Sreńscek-Nazzal, U. Narkiewicz, A. W. Morawski, R. J. Wróbel, and B. Michalkiewicz, "The increase of the micoporosity and CO2 adsorption capacity of the commercial activated carbon CWZ-22 by KOH treatment," *Microporous mesoporous Mater.*, 2016.

[42] Z. Liu, X. Zhou, F. Wu, and Z. Liu, "Microwave-Assisted Preparation of Activated Carbon Modified by Zinc Chloride as a Packing Material for Column Separation of Saccharides," *ACS omega*, vol. 5, no. 17, pp. 10106–10114, 2020.

[43] N. Bouchemal, M. Belhachemi, Z. Merzougui, and F. Addoun, "The effect of temperature and impregnation ratio on the active carbon porosity," *Desalin. water Treat.*, vol. 10, no. 1–3, pp. 115–120, 2009.

[44] K. Ho, S. Moon, H. C. Lee, Y. K. Hwang, and C. H. Lee, "Adsorptive removal of gaseous methyl iodide by triethylenediamine (TEDA)-metal impregnated activated carbons under humid conditions," *J. Hazard. Mater.*, vol. 368, pp. 550–559, 2019.

[45] S. W. Park, W. K. Lee, and H. Moon, "Adsorption and desorption of gaseous methyl iodide in a triethylenediamine-impregnated activated carbon bed," *Sep. Technol.*, vol. 3, no. 3, pp. 133–142, 1993.

[46] K. Ho, H. Chun, H.C. Lee, Y. Lee, S. Lee, H. Jung, B. Han, C-H, Lee , "Design of highly efficient adsorbents for removal of gaseous methyl iodide using tertiary amine-impregnated activated carbon: Integrated experimental and first-principles approach," *Chem. Eng. J.*, vol. 373, pp. 1003–1011, 2019.

[47] K. Ho, D. Park, M.-K. Park, and C.-H. Lee, "Adsorption mechanism of methyl iodide by triethylenediamine and quinuclidine-impregnated activated carbons at extremely low pressures," *Chem. Eng. J.*, vol. 396, p. 125215, 2020.

[48] H. Chun, J. Kang, and B. Han, "First principles computational study on the adsorption mechanism of organic methyl iodide gas on triethylenediamine impregnated activated carbon," *Phys. Chem. Chem. Phys.*, vol. 18, no. 47, pp. 32050–32056, 2016.

[49] P. Decourcière, "Evolution de la filtration des iodes dans les centrales nucléaires," in *Iodine Removal From Gaseous Effluents In The Nuclear Industry*, 1981, pp. 347–390.

[50] J. V. der M. F. Billard, A. Charamathieu, M.F. Thal, J. Caron, "Etude de l'efficacité des charbons actifs vis-à-vis de l'iodure de méthyle marqué à l'iode 131," 1966.

[51] M. Thommes, K. Kaneko, A.V. Neimark, J.P. Olivier, F. Rodriguez-Reinoso, J. Rouquerol, K. Sing "Physisorption of gases, with special reference to the evaluation of surface area and pore size distribution (IUPAC Technical Report)," *Pure Appl. Chem.*, vol. 87, no. 9–

10, pp. 1051–1069, 2015.

[52] J. Alcañiz-Monge, A. Linares-Solano, and B. Rand, “Mechanism of adsorption of water in carbon micropores as revealed by a study of activated carbon fibers,” *J. Phys. Chem. B*, vol. 106, no. 12, pp. 3209–3216, 2002.

[53] S. H. Hong, S. Jin, K. Ho, E. Hur, and C. H. Lee, “Adsorption Equilibria of Water Vapor on Surface-Modified Activated Carbons and Alumina,” *J. Chem. Eng. Data*, vol. 64, no. 11, pp. 4834–4843, 2019, doi: 10.1021/acs.jced.9b00369.

[54] D. D. Do and H. D. Do, “A model for water adsorption in activated carbon,” *Carbon N. Y.*, vol. 38, no. 5, pp. 767–773, 2000.

[55] T. Ohba, H. Kanoh, and K. Kaneko, “Structures and stability of water nanoclusters in hydrophobic nanospaces,” *Nano Lett.*, vol. 5, no. 2, pp. 227–230, 2005.

[56] F. Kepák, “Removal of gaseous fission products by adsorption,” *J. Radioanal. Nucl. Chem. Artic.*, vol. 142, no. 1, pp. 215–230, 1990.

[57] G. O. Wood and F. O. Valdez, “Nonradiometric and radiometric testing of radioiodine sorbents using methyl iodide,” in *Proceedings of the 16th DOE Nuclear Air Cleaning Conference*, 1980, pp. 448–464.